Available online at www.sciencedirect.com
SCIENCE DIRECT
Gondwana Research 9 (2006) 167 – 175
www.elsevier.com/locate/gr

Triassic paragonite- and garnet-bearing epidote-amphibolite from the Hida Mountains, Japan

T. Tsujimori [a,*], J.G. Liou [a], W.G. Ernst [a], T. Itaya [b]

[a] Department of Geological and Environmental Sciences, Stanford University, Stanford, CA 9430-2115, USA
[b] Research Institute of Natural Sciences, Okayama University of Sciences, Okayama 700-0005, Japan

Received 24 September 2004; accepted 15 March 2005
Available online 9 January 2006

Abstract

Paragonite- and garnet-bearing high-grade epidote-amphibolite (PGEA) in the Ise area of the Hida Mountains, Japan is characterized by the high-pressure (HP) epidote-amphibolite facies parageneses (M_1), garnet + hornblende + clinozoisite + paragonite + quartz + rutile. Paragonite and garnet of the peak M_1 stage are locally replaced by retrograde albite (+oligoclase) and chlorite (M_2), respectively. Phase equilibria constrain peak metamorphic conditions of $P = 1.1–1.4$ GPa and $T = 530–570$ °C, and a decompressional $P–T$ path for this rock. Mineral parageneses of prograde epidote-amphibolite facies are comparable to some HP rocks from the Hongan region of western Dabie, but differ from other HP mafic schists with cooling ages of c. 330 Ma in the Hida Mountains. New paragonite K–Ar dating for the PGEA yields a Triassic cooling event at 210 Ma that is coeval with regional cooling and exhumation of the Sulu–Dabie–Qinling (SDQ) belt. Both petrological and geochronological data of the Triassic HP epidote-amphibolite in Hida Mountains support our earlier hypothesis that the SDQ belt extends across the Korean Peninsula to SW Japan.

Keywords: Epidote-amphibolite facies; Paragonite; K–Ar age; Hida Mountains; Qinling–Dabie–Sulu belt

1. Introduction

A Triassic continental collision between the Sino-Korean and Yangtze cratons was one of the most crucial events during Phanerozoic growth of Asia. This collision produced the world largest high-pressure and ultrahigh-pressure (HP–UHP) belt (e.g., Ernst et al., 1991; Liou et al., 1996) in east-central China-the Sulu–Dabie–Qinling (SDQ) belt. This suturing event may have affected numerous tectonic and igneous activities in the present Korean Peninsula and the Japanese Islands (e.g., Isozaki, 1997; Kim et al., 2003; Oh et al., 2004). So far, numerous radiometric ages have been acquired in the SDQ belt, and have confirmed the Triassic HP–UHP formation of the orogen (e.g., Ames et al., 1993; Hacker et al., 1998, 2004); recent SHRIMP zircon U–Pb age dating combined with studies of micro-inclusions in zircon have further documented the 230 Ma prograde UHP and 210 Ma retrograde metamorphic events in Sulu (e.g., Liu et al., 2004a,b). Moreover, the timing of postmetamorphic cooling of the HP–UHP rocks at 190–210 Ma has also been confirmed by phengite $^{40}Ar–^{39}Ar$ geochronology (e.g., Eide et al., 1994; Webb et al., 1999; Hacker et al., 2000). The eastern limb of the SDQ belt may extend through the Korean Peninsula to the Japanese Islands (e.g., Ernst and Liou, 1995; Isozaki, 1997; Ishiwatari and Tsujimori, 2003; Tsujimori and Liou, 2004a). The most likely candidates for the eastern counterpart of the collisional orogen in Japan are Paleozoic HP metamorphic rocks in the Hida Mountains (Fig. 1). Recent identification of a regional eclogite-facies metamorphism in the Renge HP schist of the Hida Mountains further supports this hypothesis (Tsujimori et al., 2000a; Tsujimori, 2002). However, whether the Renge HP metamorphic rocks are related to the Triassic continental collision is still debated because of the absence of critical geochronologic evidence confirming a Triassic event; available radiometric ages for Renge HP metamorphic rocks including blueschist, eclogite and amphibolite are >100 Ma older than those of the SDQ belt.

A boulder of Triassic paragonite- and garnet-bearing epidote-amphibolite (PGEA) was recently found in the

* Corresponding author.
E-mail address: tatsukix@pangea.Stanford.EDU (T. Tsujimori).

1342-937X/$ - see front matter © 2005 International Association for Gondwana Research. Published by Elsevier B.V. All rights reserved.
doi:10.1016/j.gr.2005.03.001

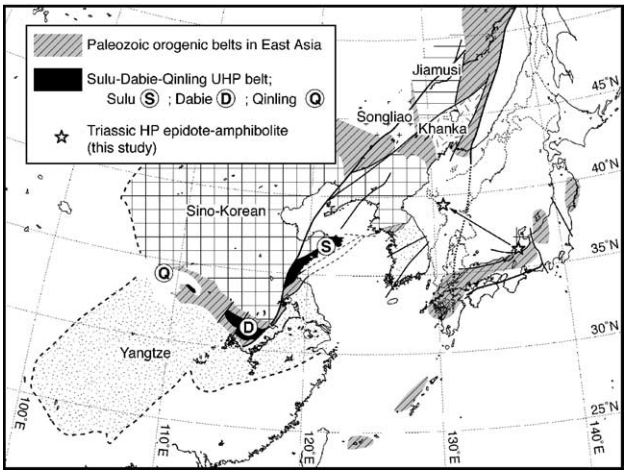

Fig. 1. Simplified geologic map of eastern Asia, showing the Chinese Triassic UP–UHP metamorphic belt (after Maruyama et al., 1994; Khanchuk, 2001).

Kuzuryu area of the Hidagaien belt (Hida marginal belt) in the Hida Mountains. As described here, petrologic features and the cooling age of the PGEA differ from other HP metamorphic rocks in the Hidagaien belt, but are similar to some HP rocks of the Sulu–Dabie terrane. We describe petrologic characteristics and the K–Ar age of the PGEA, and provide preliminary geologic implications. This is the first report of Triassic high-grade HP metamorphic rocks in the Hida Mountains.

Mineral abbreviations in this paper are after Kretz (1983); the term 'hornblende (Hbl)' describes Ca-amphibole with a dominantly hornblende composition throughout this paper.

2. Geologic outline

In the Hida Mountains of SW Japan, pre-Jurassic metamorphic rocks occur as two petrotectonic units: (1) Hida belt and (2) Hidagaien belt. These metamorphic basement terranes are unconformably overlain by Mesozoic sedimentary rocks of the Lower Jurassic Kuruma Group and the Middle Jurassic to Lower Cretaceous Tetori Group (Fig. 2).

The Hida belt consists of polymetamorphosed low- to medium-*P* orthogneiss, paragneiss, marble, amphibolite and ferro-aluminous pelitic schist, intruded calc-alkaline granitic plutons (e.g., Asami and Adachi, 1976; Inazuki, 1980; Suzuki et al., 1989; Sohma and Akiyama, 1984; Arakawa, 1990; Kano, 1991; Arakawa et al., 2000). Typical Barrovian-type aluminous pelitic schists with the assemblage Grt+Bt+Pl+St±Ky have been subdivided into the 'Unazuki schist' and the 'Hida gneiss' (Hiroi, 1983). Zircon SHRIMP U–Pb geochronology for the Hida paragneiss shows a concordant detrital age of 1841 Ma, whereas some zoned zircons record three different ages, 1690, 440, and 250 Ma (Sano et al., 2000). Microprobe Th–U-total Pb chemical ages of zircon in the Hida paragneisses yielded 230–250 Ma for sillimanite-grade amphibolite-facies metamorphism (Suzuki and Adachi, 1994). K–Ar and Rb–Sr mineral ages of both metamorphic rocks and rejuvenated Jurassic granitic intrusions are clustered at around 180 Ma (e.g., Ota and Itaya, 1989).

In contrast, the Hidagaien belt is a composite geotectonic unit that tectonically lies between the Hida belt and a Jurassic accretionary complex of the Tamba–Mino belt (e.g., Komatsu, 1990). It consists mainly of fragments of various pre-Jurassic rocks that are more widely developed in the Chugoku Mountains, SW Japan; serpentinites with blocks of Upper Paleozoic schists and Lower Paleozoic (Middle Ordovician to Upper Triassic) non-metamorphic clastic rocks are the most characteristic components (e.g., Banno, 1958; Yokoyama, 1985; Nakamizu et al., 1989; Kurihara and Sashida, 2000; Tazawa, 2004). The schists of the Hidagaien belt have been distinguished as the 'Renge schist' (e.g., Nishimura, 1998; Tsujimori et al., 2000a; Tsujimori, 2002); they records mainly greenschist- to amphibolite-facies metamorphism, and locally preserve blueschist- to eclogite-facies metamorphism. The Renge schists are roughly subdivided into two distinct groups (e.g., Banno, 1958; Tsujimori, 2002): (1) a noneclogitic unit; and (2) an eclogitic unit. Medium to coarse-grained garnet-amphibolites occur as mafic layer and lens within garnet- and biotite-bearing pelitic schists of the noneclogitic unit; they are commonly characterized by the amphibolite-facies mineral assemblage Grt+Hbl+Pl±Czo±Bt+Rt±Ilm+Qtz (e.g., Nakamizu et al., 1989). On the other hand, medium to coarse-grained eclogite and garnet-blueschist occur as mafic layers within paragonite-bearing pelitic schists of the eclogitic unit; the assemblage Grt+Omp+Gln+Czo+Rt+Qtz±Phe characterizes the eclogite-facies metamorphism (Tsujimori et al., 2000a; Tsujimori, 2002). Phengitic white micas of these Renge schists yield K–Ar and ^{40}Ar–^{39}Ar ages of around 347–283 Ma, regardless of metamorphic grade (e.g., (e.g., Shibata and Nozawa, 1968; Kunugiza et al., 2004; T. Tsujimori, unpublished data).

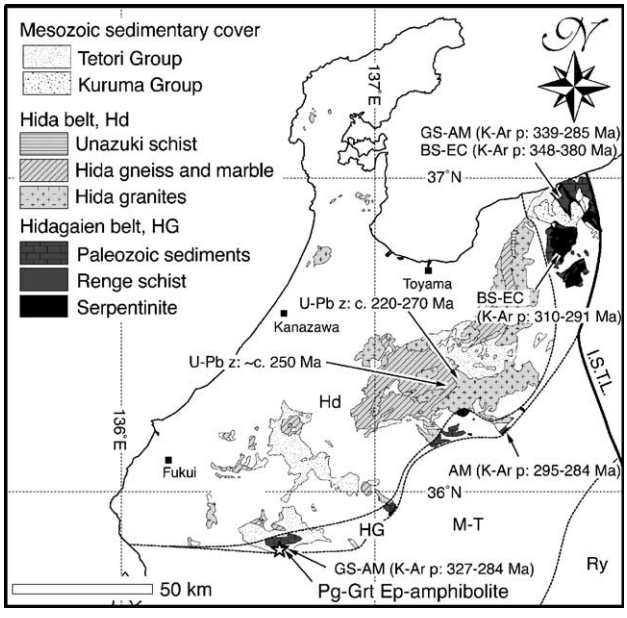

Fig. 2. Simplified geologic map of the Hida Mountains, SW Japan (after Tsujimori, 1995). Phengitic mica K–Ar ages (K–Ar p) and zircon U–Pb ages (U–Pb z) of pre-Cretaceous HP metamorphic rocks are shown; see detail in text. BS=blueschist-facies, EC=eclogite-facies, GS=greenschist-facies, AM=amphibolite-facies.

The investigated paragonite- and garnet-bearing epidote-amphibolite (PGEA) was collected as a river boulder (40 × 40 cm in size) in a branch of the Ise River, Kuzuryu area (Fig. 2). A similar boulder of 'garnet–epidote–hornblende schist' from the same area was descried by Miyakawa (1982), who did not identify paragonite. In this area, a fault-bounded, noneclogitic Renge schist body (4 × 2 km), called the 'Ise body', is associated with Permian volcanoclastic rocks of the Konogidani Formation, and serpentinites with minor deformed diorite (Yamada, 1967; Miyakawa, 1982; Kurihara, 2003). The Ise body consists mainly of greenschist- to amphibolite-facies mafic and pelitic schists. Mafic schist contains the mineral assemblage Act+Ep+Chl+Ttn+Ab+Qtz, and pelitic schist is characterized by the assemblage Phe+Bt±Grt+Ab+Qtz+Ttn (Miyakawa, 1982). The pelitic schist gives phengite K–Ar ages of 327–314 Ma (Kunugiza et al., 2004), and a deformed diorite yields hornblende K–Ar ages of 415–397 Ma (Shibata et al., 1980). Although the relationship between the PGEA and greenschist-facies schists of the Ise body is unclear, the PGEA may have originally been a tectonic inclusion within adjacent serpentinites.

3. Petrography

The PGEA is a well-foliated, medium-grained mafic rock; garnet porphyroblasts, up to 5 mm in size are scattered in the foliated matrix (Fig. 3a). The latter consists mainly of

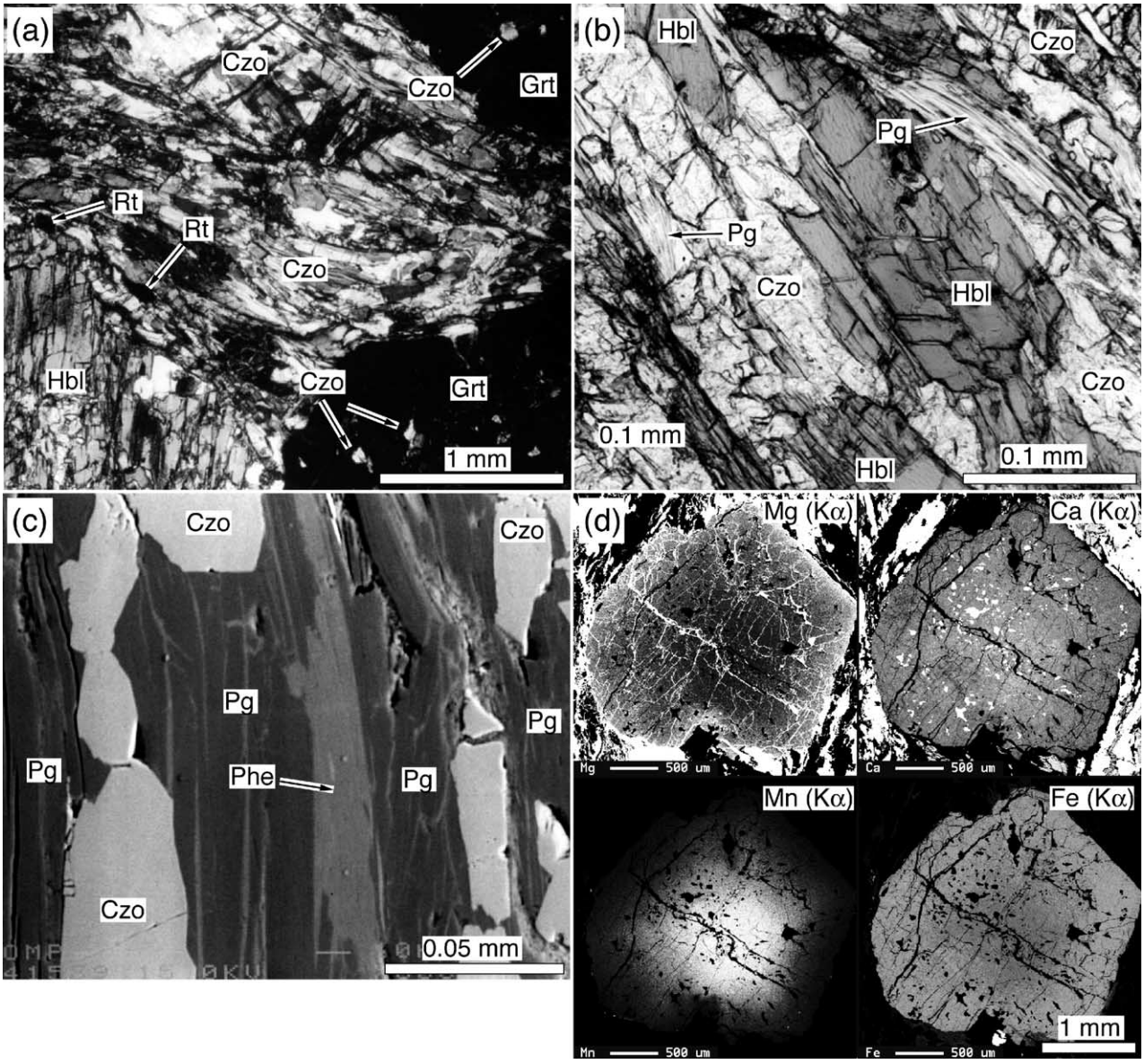

Fig. 3. Photomicrographs showing microtextures of investigated samples. (a) Cross-polarizer view of garnet and porphyroclastic hornblende; porphyroclastic hornblende is enveloped around bya foliated mosaic aggregate of clinozoisite. (b) Open-polarizer view of paragonite and nematoblastic hornblende that defines the foliation. (c) Back-scattered electron image of paragonite with minor phengite. (d) X-ray images (Mg, Ca, Mn, and Fe) of garnet, showing prograde chemical zoning. Brighter color represents higher concentration.

hornblende, garnet, clinozoisite and paragonite, with small amounts of quartz, albite (rare oligoclase), phengite, and rutile. Apatite and chlorite are accessories. Foliation is defined by preferred orientation of nematoblastic hornblende and paragonite (Fig. 3b). Mosaic aggregates of clinozoisite are intergrown with paragonite, hornblende and rutile. Minor phengite coexists with paragonite in the matrix (Fig. 3c). Garnet porphyroblasts contain inclusions of clinozoisite, rutile, quartz and rare paragonite. Most acicular hornblende grains (<1 mm in length) are arranged roughly parallel to the schistosity; some coarse-grained hornblende porphyroclasts (2–4 mm in size) are wrapped around by layers of mosaic aggregates of clinozoisite (Fig. 3a) and nematoblastic hornblende. Such textural relations indicate that relict, coarse-grained hornblende underwent grain-size reduction by recrystallization during deformation. The hornblende porphyroclasts contain quartz and rutile inclusions.

Petrographic relations indicate that the investigated PGEA experienced at least two stages of metamorphic recrystallization: a peak epidote-amphibolite stage (M_1) and retrograde stages (M_2). Except for some hornblende porphyroclasts, foliated matrix minerals and garnet porphyroblasts are thought to be in textural equilibrium, and the assemblage Grt+Hbl+Czo+Pg±Phe+Rt+Qtz characterizes the M_1 peak metamorphic stage; M_1 garnet records prograde chemical zoning (Fig. 3d). Albite and oligoclase occur as later M_2 stage minerals that rarely replace M_1 paragonite. Furthermore, M_2 chlorite fills minor cracks in the garnet porphyroblasts.

4. Mineral chemistry

Electron microprobe analysis was carried out with a JEOL JXA-8900R at Okayama University of Science. Quantitative analyses were performed at 15 kV accelerating voltage, 12 nA beam current and a 3 μm beam size. Natural and synthetic silicates and oxides were used as standards. The ZAF (oxide basis) method was employed for matrix corrections. Representative analyses of rock-forming minerals are listed in Table 1.

4.1. Garnet

Garnets are characterized by high almandine (Alm) components with moderate grossular (Grs) and low pyrope (Pyr) and spessartine (Sps) (Alm=58–66%, Grs=20–26%, Pyr=5–15%, Sps=2–13%; Fig. 4). They show distinct prograde chemical zoning in $Mg/(Mg+Fe^{2+})$ atomic ratio [$=X_{Mg}$], ranging from 0.08 to 0.19; grossular and spessartine decrease toward the rim (Fig. 4). Compared with garnet composites of other Renge noneclogitic and eclogitic mafic schists, the garnet in this rock contains garnets of lower grossular and spessartine contents.

4.2. Hornblende

The Fe^{2+}/Fe^{3+} ratios of amphiboles were estimated on the anhydrous basis of 23 oxygens p.f.u, and assuming a cation total of 13 excluding Ca, Na and K. M_1 neoblastic hornblendes

Table 1
Representative electron-microprobe analyses of rock-forming minerals in the PGEA

	Garnet		Honeblende			Clinozoisite		Paragonite	Phnegite
	Core	Rim	PC				Inc.		
SiO_2	37.03	36.95	43.30	45.86	55.99	38.50	38.56	46.93	49.38
TiO_2	0.03	0.01	0.43	0.16	0.04	0.00	0.04	0.00	0.07
Al_2O_3	20.82	21.07	16.09	13.17	10.74	26.92	27.89	38.88	31.69
Cr_2O_3	0.00	0.00	0.00	0.00	0.04	0.00	0.00	0.01	0.00
FeO*	27.93	30.77	14.25	14.64	6.46	8.45	7.12	0.51	1.57
MnO	4.99	0.99	0.02	0.01	0.00	0.11	0.29	0.00	0.04
MgO	1.37	3.74	9.78	11.24	6.83	0.10	0.06	0.07	1.89
CaO	8.49	7.15	10.64	9.47	11.74	22.93	23.24	0.60	0.05
Na_2O	0.04	0.00	2.81	2.85	8.03	0.01	0.05	6.97	1.01
K_2O	0.01	0.01	0.13	0.10	0.00	0.00	0.02	1.15	9.09
Total	100.70	100.68	97.45	97.50	99.87	97.02	97.27	95.13	94.78
O=	12	12	23	23	23	12.5	12.5	11	11
Si	3.007	2.981	6.318	6.574	6.221	3.008	2.999	3.014	3.275
Ti	0.010	0.004	0.047	0.043	0.044	0.000	0.002	0.000	0.004
Al	1.993	2.004	2.767	2.225	2.714	2.478	2.557	2.943	2.477
Cr	0.000	0.000	0.000	0.000	0.002	0.000	0.000	0.001	0.000
Fe^{3+}			0.358	0.820	0.755	0.552	0.463		
Fe^{2+}	1.725	1.887	1.381	0.935	1.094			0.028	0.087
Mn	0.343	0.068	0.003	0.001	0.016	0.007	0.019	0.000	0.002
Mg	0.166	0.450	2.126	2.401	2.155	0.011	0.007	0.006	0.187
Ca	0.739	0.618	1.663	1.454	1.568	1.919	1.937	0.041	0.004
Na	0.005	0.000	0.795	0.793	0.836	0.001	0.007	0.868	0.129
K	0.001	0.000	0.025	0.018	0.029	0.000	0.002	0.094	0.769
Total	7.989	8.013	15.482	15.266	15.432	7.977	7.993	6.995	6.933
X_{Mg}	0.09	0.19	0.61	0.72	0.66	1.00	1.00	0.19	0.68

FeO*=total Fe as FeO. $X_{Mg}=Mg/(Mg+Fe^{2+})$.
PC=porphyroclast; Inc.=inclusion in garnet.

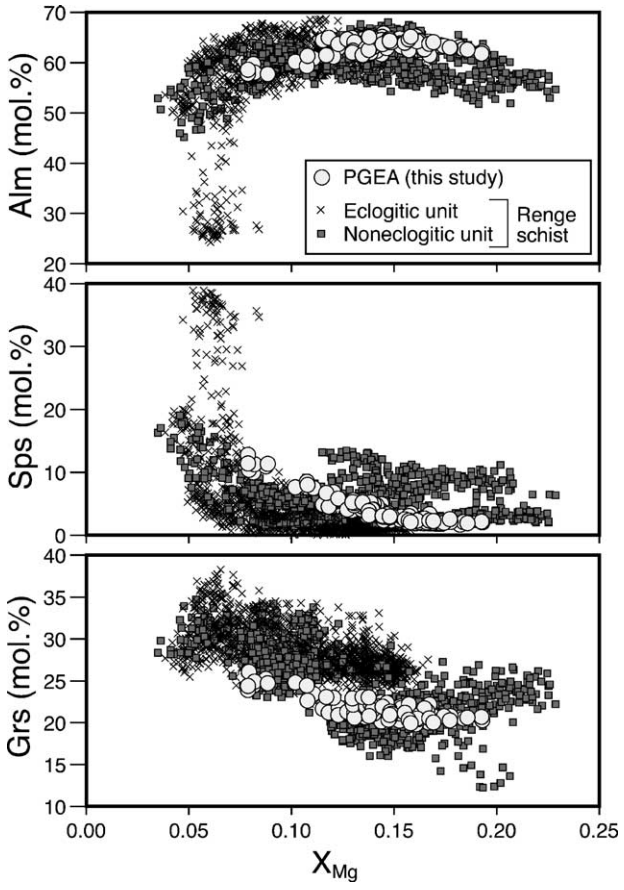

Fig. 4. Chemical compositions of garnet in X_{Mg} versus Alm, Pyr, and Sps components. For comparisons, garnets from the Renge HP schists in the Hida Mountains are also plotted.

range in composition from hornblende to rare barroisite (Fig. 5), with Si=6.2–6.6 p.f.u., $^{[B]}$Na (Na in the B-site)=0.37–0.56, and $^{[A]}$(Na+K)=0.11–0.43; X_{Mg} ranges from 0.61 to 0.82. Al_2O_3 content reaches 15.9 wt.% and typically decreases at the rim. Porphyroclastic hornblendes, classified as hornblende and tschermakite, have Si=6.2–6.5 p.f.u., $^{[B]}$Na=0.34–0.41, and $^{[A]}$(Na+K)=0.26–0.48; X_{Mg} ranges from 0.61 to 0.74. Because porphyroclastic hornblendes may have been recrystallized, they show a similar compositions to those of neoblastic hornblendes. The compositional trend of hornblende in the PGEA is roughly similar to those of noneclogitic unit schists. However, the $^{[A]}$(Na+K) value of hornblende does not exceed 0.5 in the Ise River boulder.

4.3. Other minerals

Clinozoisite as mosaic aggregates in the matrix is characterized by X_{Fe3+}[=$Fe^{3+}/(Fe^{3+}Al)$] values ranging from 0.12 to 0.22; clinozoisite inclusions in garnet have X_{Fe3+} of 0.13–0.19.

Paragonite in the matrix ranges in Na/(Na+K) ratio from 0.88 to 0.94, and coexisting phengite has the composition Na/(Na+K)=0.14–0.17 and Si p.f.u.=3.2–3.3.

M_2 albite and oligoclase that replace paragonite have 0–5% and 15–19% anorthite (An) component, respectively.

X_{Mg} of chlorite ranges from 0.57 to 0.64.

5. *P–T* conditions of metamorphism

The prograde epidote-amphibolite facies stage (M_1) produced the assemblage Grt+Hbl+Czo+Pg±Phe+Rt+Qtz. *P–T* conditions for the Pg+Czo+Qtz assemblage can be defined by the following experimentally determined reactions (Fig. 6):

$$\text{Lws} + \text{Ab(or Jd)} = \text{Zo} + \text{Pg} + \text{Qtz} + \text{H}_2\text{O} \quad (1)$$

(Heinrich and Althaus, 1988), and

$$\text{Zo} + \text{Pg} + \text{Qtz} = \text{Mrg} + \text{Pl} \quad (2)$$

(Franz and Althaus, 1977).

The absence of either blueschist- or eclogite-facies assemblages together with the reactions (1) and (2) indicates an approximate epidote-amphibolite facies *P–T* condition of *P*=1.1–1.4 GPa and *T*=530–570 °C, at pressures just below those of the eclogite facies (Fig. 6). Moreover, the

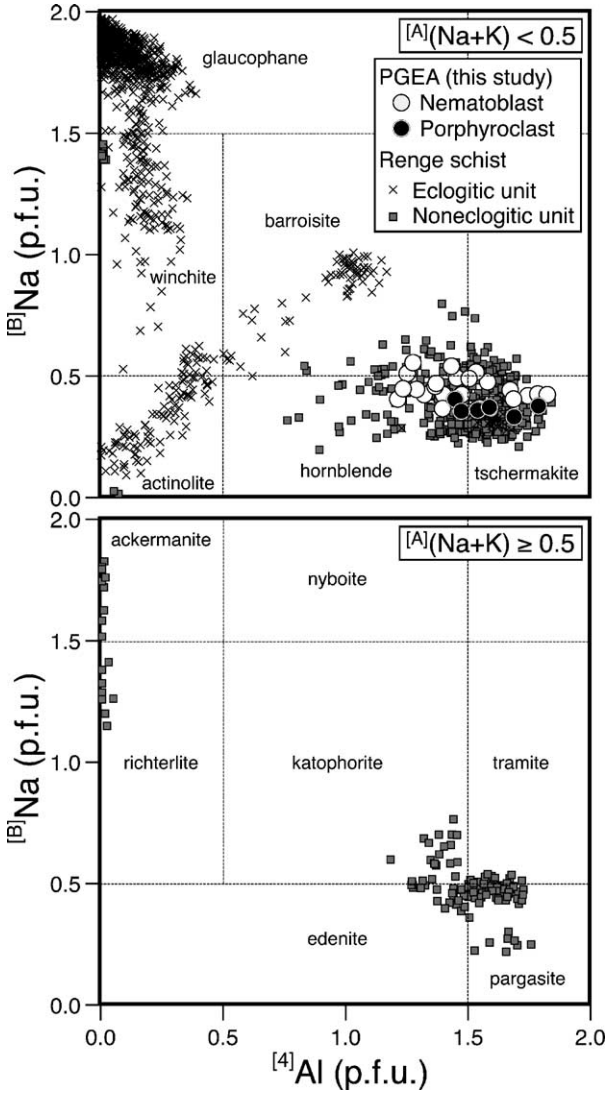

Fig. 5. Chemical compositions of hornblende in Na_B versus Al^{IV} diagrams. For comparisons, amphiboles from the Renge HP schists in the Hida Mountains are also plotted.

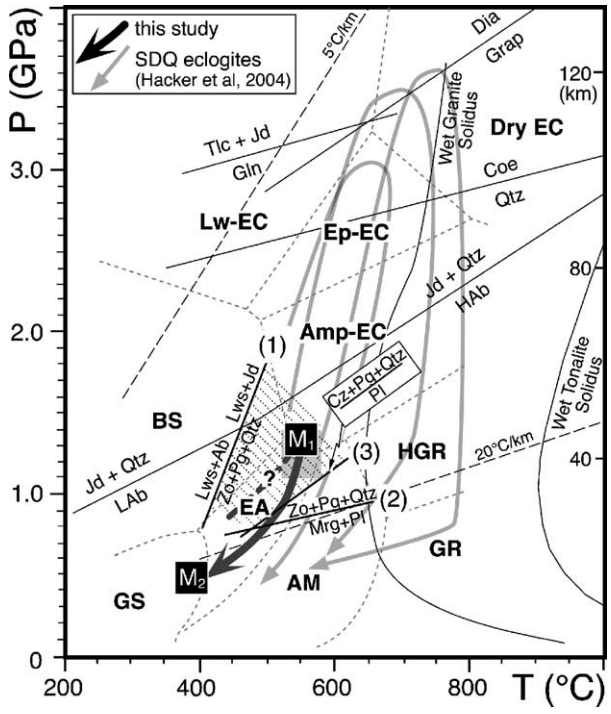

Fig. 6. $P-T$ diagram showing a qualitative metamorphic condition for the peak M_1 stage (gray area), and the retrograde $P-T$ path, from M_1 to M_2 for the PGEA. Reactions curves (1) and (2) define to lower $P-T$ limit for the stability field of the Zo (Czo)+Pg assemblage (shaded area). For comparisons, the inferred $P-T$ paths of the SQD eclogites (Hacker et al., 2004) are also shown. The metamorphic facies and their abbreviations, and phase equilibria are after Liou et al. (2004).

relatively high Al (up to 17.5 wt.% Al_2O_3) and moderate Na (up to 3.0 wt.%) contents of hornblende and the presence of rutile instead of titanite and ilmenite further support HP conditions for the M_1 stage (Ernst and Liu, 1998; Liu et al., 1996).

Furthermore, the decompressional paragonite-breakdown reaction to form M_2 sodic plagioclase can be written as:

$$Pg + Czo + Qtz = An + Ab + H_2O. \quad (3)$$

This reaction constrains a lower pressure limit for the M_1 assemblage; the minimum pressure calculated using THERMOCALC (ver. 3.21) program (Powell et al., 1998) with analyzed mineral compositions is $P=1.0$ GPa at $T=550$ °C (Fig. 6).

The paragonite-bearing assemblage in amphibolitic rocks is one of the critical assemblages to constrain HP metamorphism. Konzett and Hoinkes (1996) calculated the stability of Pg+Hbl (tschermakite), and suggested that this assemblage is stable at pressures below the omphacite stability field. This suggestion is also supported by other calculations (e.g., Molina and Poli, 1998). In fact, the Hbl+Pg assemblage has been described as a retrograde mineral assemblage for some Dabie–Sulu UHP eclogites (e.g., Okay, 1995; Mattinson et al., 2004). The retrograde M_2 stage represents minor greenschist-facies overprinting after the peak HP metamorphism. The appearance of sodic plagioclase replacing M_1 paragonite indicates that the retrograde $P-T$ trajectory crossed reaction (3) to greenschist-facies $P-T$ conditions.

6. Age of metamorphism

A paragonite separate from the investigated PGEA was used for conventional K–Ar dating at Okayama University of Science. The separate was treated with 2N HCl to dissolve out chlorite along cleavage planes, and was cleaned at 80 °C with ion-exchanged water. ^{40}K was analyzed by flame photometry using a 2000 ppm Cs buffer. Ar isotopic compositions were measured on a 15 cm radius sector-type HIRU mass-spectrometer; an accurately measured amount of ^{38}Ar gas was used as a spike (Nagao et al., 1984; Itaya et al., 1991). Decay constants for ^{40}K to ^{40}Ar and ^{40}Ca, and the ^{40}K abundance used in to age calculation are 0.581×10^{-10}/yr, 4.962×10^{-10}/yr, and 0.0001167, respectively (Steigher and Jäger, 1977).

The paragonite K–Ar age of the PGEA boulder yields 210.6±4.6 Ma (Table 2). Because paragonite grew during the HP metamorphism, this age is considered to reflect the time at which the PGEA cooled below the K–Ar closure temperature of paragonite. Although there is no experimental determination of ^{40}Ar diffusion in paragonite, it has been generally accepted that its K–Ar closure temperature is similar to that for muscovite at 420±50 °C (e.g., Konzett and Hoinkes, 1996; Marshall et al., 1998; Schneider et al., 2004). The K–Ar closure temperature of paragonite can be supported by a good agreement between paragonite ^{40}Ar–^{39}Ar age (52.3 Ma) and low-Th/U metamorphic zircon U–Pb age (52.4 Ma) from a HP metagabbro from Synos (Tomaschek et al., 2003). Moreover, recent in situ ^{40}Ar–^{39}Ar laserprobe dating of metamorphic white micas in Barrovian-type schist from the

Table 2
K–Ar ages of the PGEA and Renge schists from the Ise area

Sample	K (wt.%)	Rad.^{40}Ar (10^{-8} cc STP/g)	Non-rad. Ar (%)	Age (Ma)
Paragonite-bearing garnet–epidote-amphibolite boulder (this study)				
PGEA [Pg]	0.573±0.01	497.0±5.8	6.3	210.6±4.6
Renge pelitic schists of Ise body				
IS-PS01 [Phe] (TT)	6.03±0.12	7974±84	4.5	312.3±6.5
IS0723 [Phe] (K97)	4.38±0.09	6030±62	1.2	322.7±6.7
IS0732 [Phe] (K97)	4.12±0.08	5724±57	1.2	327.0±6.7
IS0735 [Phe] (K97)	5.49±0.11	7360±84	1.3	313.7±6.6

Pg=paragonite; Phe=phengite; TT=unpublished data; K9=Kunugiza et al. (1997).

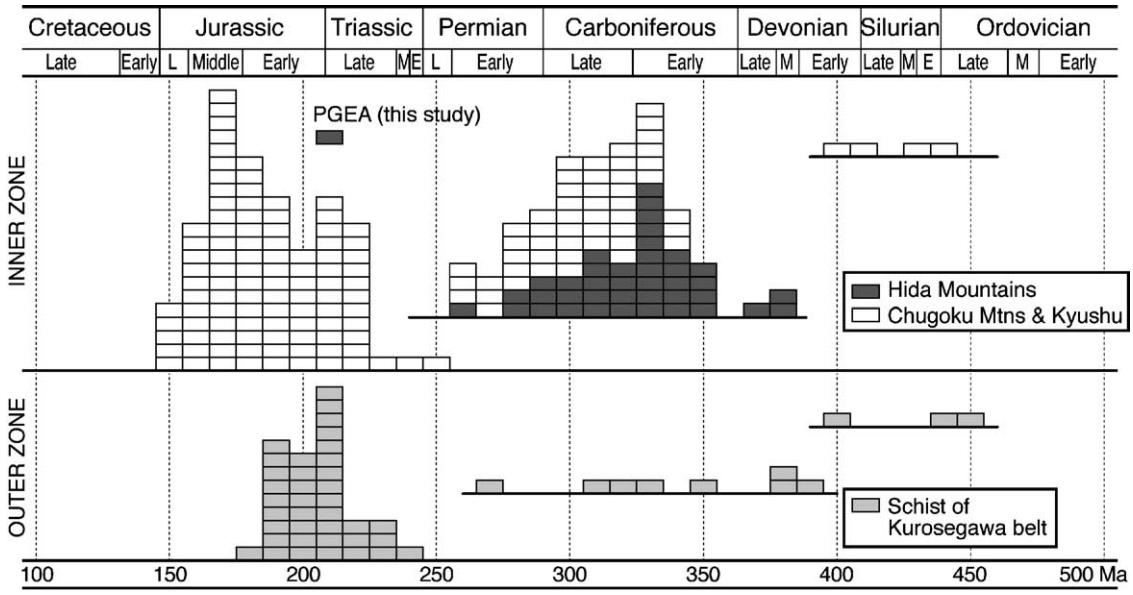

Fig. 7. Frequency distribution of K–Ar and Rb–Sr mineral ages of pre-Cretaceous HP metamorphic rocks in the Inner Zone (Hida Mountains, Chugoku Mountains, and Kyushu) and the Outer Zone (Kurosegawa belt, Shikoku) of SW Japan. Data are from Shibata and Nozawa (1968), Maruyama and Ueda (1974), Maruyama et al. (1978), Shibata and Ito (1978), Suzuki et al. (1990), Nishimura et al. (1989), Isozaki and Itaya (1990), Isozaki and Itaya (1991), Kabashima et al. (1995), Kunugiza et al. (2004), Nishimura (1998), and Tsujimori and Itaya (1999). Unpublished K–Ar and Ar–Ar data (one Suo schist and twenty-three Renge schists) of T. Tsujimori are also included in the diagram. All data except for hornblende ages of the kyanite-bearing epidote-amphibolite (Tsujimori et al., 2000b; Tsujimori and Liou, 2004b) are phengitic mica ages. Time scale is after Harland et al. (1990).

Variscan belt revealed relatively high K–Ar closure temperatures (>500 °C) of white micas (Di Vincenzo et al., 2004). Considering these, the paragonite K–Ar age of 210 Ma is interpreted as the time of postmetamorphic cooling soon after the metamorphic peak (as is the case for the SDQ belt, e.g., Hacker et al., 2000). The observed minor retrogression support this interpretation.

7. Geologic implications

The finding of a Triassic HP metamorphic rock in the Japanese Paleozoic terrane is significant in terms of the regional tectonic framework of Eastern Asia. Our petrologic work has documented an HP epidote-amphibolite facies metamorphism in the PGEA from the Hida Mountains; the paragonite-bearing HP epidote-amphibolite facies mineral assemblage has not been previously described in HP mafic metamorphic rocks in this belt. Moreover, paragonite K–Ar dating of the PGEA confirms a Triassic cooling event that is clearly younger than prior age data for HP metamorphic rocks in the Hida Mountains (Fig. 7); cooling ages of the Renge HP schists converge around 330 Ma. Although pumpellyite–actinolite-to-greenschist/blueschist transitional facies rocks occur in the Triassic–Jurassic Suo HP metamorphic belt of the Chugoku Mountains (e.g., Nishimura et al., 1989; Nishimura, 1998), the PGEA differs substantially from these low-grade metamorphic rocks. Considering petrologic and geochronologic features, the investigated PGEA may represent an exotic fragment from a regional Triassic high-grade HP metamorphic unit.

What is the significance of our finding of Triassic HP epidote-amphibolite facies metamorphism in the Hida Mountains? Prograde paragonite- and garnet-bearing HP epidote-amphibolite is generally restricted to the epidote-amphibolite/eclogite transitional facies (e.g., Konzett and Hoinkes, 1996; Molina and Poli, 1998). In the Hong'an region of western Dabie, a prograde zonation from blueschist/greenschist transitional through epidote-amphibolite and quartz-eclogite to coesite-eclogite zone is well documented as the best representative petrotectonic assemblages for Triassic subduction of the Yangtze plate beneath the Sino-Korean craton (Liou et al., 1996; Eide and Liou, 2000; Liu et al., 2004a,b; Liu and Ye, 2004). Each metamorphic zone may have a similar P–T gradient, but was subducted to different depths. The prograde paragonite-bearing mineral assemblage Grt+Hbl+Czo+Pg+Qtz+Rt has been described as a precursor of eclogite-facies rocks (e.g., Liu and Ye, 2004). A similar prograde transition has also been documented in the southern Sulu belt. For instance, Enami and Nagasaki (1999) described the prograde epidote-amphibolite facies mineral inclusions pargasite, clinozoisite, paragonite, staurolite, and margarite from the cores of zoned garnets in Sulu UHP eclogites. Although staurolite and margarite have not been found in our PGEA, the Hbl+Pg+Czo assemblage is comparable to the precursor assemblage of the Sulu UHP eclogite.

It is obvious that the investigated PGEA underwent neither UHP metamorphism nor eclogite-facies metamorphism. However, this PGEA may be an equivalent to HP rocks recrystallized at shallower subduction depths and exhumed; some are preserved as inclusions in HP–UHP eclogites of the Chinese Triassic SDQ belt. Our new finding of Triassic HP epidote-amphibolite facies metamorphism supports an early speculation regarding the eastern extension of the suture zone (Ernst and Liou, 1995); the SDQ belt may well extend to SW Japan.

Acknowledgments

This research was supported financially in part by the Japanese Society for the Promotion of Science Research Fellowship for Research Abroad of the first author. This manuscript was prepared with support by NSF EAR-0003355 and EAR-0510325. Preparation of this manuscript was supported by Open Research Center, Okayama University of Science (contribution to ORC no. 1). We thank T. Okada for his help in the age dating. The authors wish to acknowledge careful review by C.W Oh, S.W. Kim, and H. Hokada.

References

Ames, L., Tilton, G.R., Zhou, G., 1993. Timing of collision of the Sino-Korean and Yangtze cratons; U–Pb zircon dating of coesite-bearing eclogite. Geology 21, 339–342.

Arakawa, Y., 1990. Two types of granitic intrusions in the Hida belt, Japan: Sr isotopic and chemical characteristics of the Mesozoic Funatsu granitic rocks. Chem. Geol. 85, 101–117.

Arakawa, Y., Saito, Y., Amakawa, H., 2000. Crustal development of the Hida belt, Japan: evidence from Nd–Sr isotopic and chemical characteristics of igneous and metamorphic rocks. Tectonophysics 328, 183–204.

Asami, M., Adachi, M., 1976. Staurolite-bearing cordierite–sillimanite gneiss from the Toga area in the Hida metamorphic terrane, central Japan. J. Geol. Soc. Japan 82, 259–271.

Banno, S., 1958. Glaucophane schists and associated rocks in the Omi district, Niigata Prefecture, Japan. Jpn. J. Geol. Geogr. 29, 29–44.

Di Vincenzo, G., Carosi, R., Palmeri, R., 2004. The relationship between tectonometamorphic evolution and argon isotope records in white mica: constraints from in situ $^{40}Ar-^{39}Ar$ laser analysis of the Variscan basement of Sardinia. J. Petrol. 45, 1013–1043.

Eide, E.A., Liou, J.G., 2000. High-pressure blueschists and eclogites in Hong'an: a frame work for addressing the evolution of high- and ultrahigh-pressure rocks in central China. Lithos 52, 1–22.

Eide, E.A., McWilliam, M.O., Liou, J.G., 1994. $^{40}Ar/^{39}Ar$ geochronology and exhumation of high-pressure to ultrahigh-pressure metamorphic rocks in east central China. Geology 22, 601–604.

Enami, M., Nagasaki, A., 1999. Prograde $P-T$ path of kyanite eclogites from Junnan in the Sulu ultrahigh-pressure province, eastern China. Isl. Arc 8, 459–474.

Ernst, W.G., Liou, J.G., 1995. Contrasting plate-tectonic styles of the Qinling–Dabie–Sulu and Franciscan metamorphic belts. Geology 23, 353–356.

Ernst, W.G., Liu, J., 1998. Experimental phase-equilibrium study of Al- and Ti-contents of calcic amphibole in MORB—a semiquantitative thermobarometer. Am. Mineral. 83, 952–969.

Ernst, W.G., Zhou, G., Liou, J.G., Eide, E., Wang, X., 1991. High-pressure and superhigh-pressure metamorphic terranes in the Qinling–Dabie mountain belt, central China; Early- to Mid-Phanerozoic accretion of the western Paleo-Pacific rim. Pac. Sci. Ass. Info. Bull. 43, 6–15.

Franz, G., Althaus, E.K., 1977. The stability relations of paragenesis paragonite–zoisite–quartz. News. Jahrb. Mineral. Abh. 130, 159–167.

Hacker, B.R., Ratschbacher, L., Webb, L., Ireland, T., Walker, D., Dong, S., 1998. U/Pb zircon ages constrain the architecture of the ultrahigh-pressure Qinling–Dabie Orogen, China. Earth Planet. Sci. Lett. 161, 215–230.

Hacker, B.R., Ratschbacher, L., Webb, L.E., McWilliams, M., Calvert, A., Dong, S., Wenk, H.-R., Chateigner, D., 2000. Exhumation of ultrahigh-pressure rocks in east-central China: Late Triassic–Early Jurassic tectonic unroofing. J. Geophys. Res. 105, 13339–13364.

Hacker, B.R., Ratschbacher, L., Liou, J.G., 2004. Subduction, collision, and exhumation in the Qinling–Dabie Orogen. In: Malpas, J., Fletcher, C.J.N., Ali, J.R., Aitchison, J.C. (Eds.), Aspect of the Tectonic Evolution of China, Geol. Soc. London, Special Publ., vol. 226, pp. 157–175.

Harland, W.B., Armstrong, R.L., Cox, A.V., Craig, L.E., Smith, A.G., Smith, D.G., 1990. A Geologic Time Scale 1989. Cambridge Univ. Press, Cambridge. 263 pp.

Heinrich, W., Althaus, E., 1988. Experimental determination of reactions 4 lawsonite+1 albite=1 paragonite+2 zoisite+2 quartz+6 H_2O and 4 lawsonite+1 jadeite=1 paragonite+2 zoisite+1 quartz+6 H_2O. Neues Jahrb. Mineral. Monatsh. H11, 516–528.

Hiroi, Y., 1983. Progressive metamorphism of the Unazuki pelitic schists in the Hida terrane, central Japan. Contrib. Mineral. Petrol. 82, 334–350.

Inazuki, T., 1980. Metamorphism of calc-siliceous rocks in the Momose–Mizunashi district, Hida metamorphic belt, central Japan. J. Geol. Soc. Japan 86, 727–740 (in Japanese with English abst.).

Ishiwatari, A., Tsujimori, T., 2003. Paleozoic ophiolites and blueschists in Japan and Russian Primorye in the tectonic framework of East Asia: a synthesis. Isl. Arc 12, 190–206.

Isozaki, Y., 1997. Contrasting two types of orogen in Permo-Triassic Japan: accretionary versus collisional. Isl. Arc 6, 2–24.

Isozaki, Y., Itaya, T., 1990. K–Ar ages of weakly metamorphosed rocks at the northern margin of Kurosegawa terrane in central Shikoku and western Kii Peninsula — extent of the Kurosegawa Terrane in southwest Japan. J. Geol. Soc. Japan 96, 623–639 (in Japanese with English abst.).

Isozaki, Y., Itaya, T., 1991. Pre-Jurassic kippe in northern Chichibu belt in west-central Shikoku, southwest Japan. Kurosegawa terrane as a tectonic outlier of the pre-Jurassic rocks on the Inner Zone. J. Geol. Soc. Japan 97, 431–450 (in Japanese with English abst.).

Itaya, T., Nagao, K., Inoue, K., Honjyou, Y., Okada, T., Ogata, A., 1991. Argon isotopic analysis by a newly developed mass spectrometric system for K–Ar dating. Mineral. J. 15, 203–221.

Kabashima, T., Isozaki, Y., Nishimura, Y., Itaya, T., 1995. Re-examination on K–Ar ages of the Kiyama high-P/T schists in central Kyushu. J. Geol. So. Japan 101, 397–400 (in Japanese).

Kano, T., 1991. Metasomatic origin of augen gneiss and related mylonitic rocks in the Hida metamorphic complex, central Japan. Mineral. Petrol. 45, 29–45.

Kim, C-.B., Chang, H-.W., Turek, A., 2003. U–Pb zircon ages and Sr–Nd–Pb isotopic compositions for Permian–Jurassic plutons in the Ogcheon belt and Ryeongnam massif, Korea: tectonic implications and correlation with the China Qinling–Dabie belt and the Japan Hida belt. Isl. Arc 12, 366–382.

Khanchuk, A.I., 2001. Pre-Neogene tectonics of the Sea-of-Japan region. A view from the Russian side. Earth Sci. (Chikyu Kagaku) 55, 275–292.

Komatsu, M., 1990. Hida "Gaien" Belt and Joetsu Belt. In: Ichikawa, K., Mizutani, S., Hara, I., Hada, S., Yao, A. (Eds.), Pre-Cretaceous Terranes of Japan. Publication of IGCP Project No. 224: Pre-Jurassic Evolution of Eastern Asia, Osaka, pp. 25–40.

Konzett, J., Hoinkes, G., 1996. Paragonite–hornblede assemblages and their petrological significance: an example from the Austroalpine Schneeberg Complex, Southern Tyrol, Italy. J. Metamorph. Geol. 14, 85–101.

Kretz, R., 1983. Symbols for rock forming minerals. Am. Mineral. 68, 277–279.

Kunugiza, K., Goto, A., Itaya, T., Yokoyama, K., 2004. Geological development of the Hida Gaien belt: constraints from K–Ar ages of high P/T metamorphic rocks and U–Th–Pb ages of granitic rocks affecting contact metamorphism of serpentinite. J. Geol. Soc. Japan 110, 580–590 (in Japanese with English abst.).

Kurihara, T., Sashida, K., 2000. Taxonomy of Late Silurian to Middle Devonian radiolarians from the Kuzuryu lake district of the Hida Gaien Belt, Fukui Prefecture, central Japan. Micropaleontology 46, 51–71.

Kurihara, T., 2003. Stratigraphy and geologic age of the Middle Paleozoic strata in the Kuzuryu Lake–Upper Ise River area of the Hida–Gaien Terrane, central Japan. J. Geol. Soc. Japan 109 (8), 425–441 (in Japanese with English abst.).

Liou, J.G., Zhang, R.Y., Eide, E.A., Maruyama, S., Wang, X., Ernst, W.G., 1996. Metamorphism and tectonics of high-P and ultrahigh-P belts in Dabie–Sulu regions, eastern central China. In: Yin, A., Harrison, T.M. (Eds.), The Tectonic Evolution of Asia. Cambridge Univ. Press, New York, pp. 330–343.

Liou, J.G., Tsujimori, T., Zhang, R.Y., Katayama, I., Maruyama, S., 2004. Global UHP metamorphism and continental subduction/collision: the Himalayan model. Int. Geol. Rev. 46, 1–27.

Liu, J., Ye, K., 2004. Transformation of garnet epidote amphibolite to eclogite, western Dabie Mountains, China. J. Metamorph. Geol. 22, 383–394.

Liu, J., Bohlen, S.R., Ernst, W.G., 1996. Stability of hydrous phases in subducting oceanic crust. Earth Planet. Sci. Lett. 143, 161–171.

Liu, F., Xu, Z., Liou, J.G., Song, B., 2004a. SHRIMP U–Pb ages of ultrahigh-pressure and retrograde metamorphism of gneisses, south-western Sulu terrane, eastern China. J. Metamorph. Geol. 22, 315–326.

Liu, X., Wei, C., Dong, S., Liou, J., 2004b. Thermobaric structure of a traverse across western Dabieshan: implications for collision tectonics between the Sino-Korean and Yangtze cratons. J. Metamorph. Geol. 22, 361–379.

Marshall, D., Pfeifer, H.R., Hunziker, J.C., Kirschner, A., 1998. A pressure–temperature–time path for the NE Mont-Blanc massif: fluid-inclusion, isotopic and thermobarometric evidence. Eur. J. Mineral. 10, 1227–12240.

Maruyama, S., Ueda, Y., 1974. Schist xenolith in ultrabasic body accompanied with Kurosegawa tectonic zone in eastern Shikoku and their K–Ar ages. J. Japan. Ass. Mineral. Petrol. Econ. Geol. 70, 42–52 (in Japanese with English abst.).

Maruyama, S., Ueda, Y., Banno, S., 1978. 208–240 M.Y. old jadeite-glaucophane schists in the Kurosegawa tectonic zone near Kochi City, Shikoku. J. Japan. Ass. Mineral. Petrol. Econ. Geol. 73, 300–310.

Maruyama, S., Liou, J.G., Zhang, R.Y., 1994. Tectonic evolution of the ultrahigh-pressure (UHP) and high-pressure (HP) metamorphic belts from central China. Isl. Arc 3, 112–121.

Mattinson, C.G., Zhang, R.Y., Tsujimori, T., Liou, J.G., 2004. Epidote-rich talc–kyanite–phengite eclogites, Sulu terrane, eastern China: $P–T–fO_2$ estimations and the significance of the epidote–talc assemblage in eclogite. Am. Mineral. 22, 1772–1783.

Miyakawa, K., 1982. Low-grade metamorphic rocks of the Hida marginal belt in the upper Kuzuryu river area, central Japan. J. Assoc. Petrol. Mineral. Econ. Geol. 77, 256–265 (in Japanese with English abst.).

Molina, J.F., Poli, S., 1998. Singular equilibria in paragonite blueschists, amphibolites and eclogites. J. Petrol. 39, 1325–1346.

Nakamizu, M., Okada, M., Yamazaki, T., Komatsu, M., 1989. Metamorphic rocks in the Omi–Renge serpentinite melange, Hida Marginal Tectonic Belt, Central Japan. Mem. Geol. Soc. Japan (33), 21–35 (in Japanese with English abst.).

Nagao, K., Nishido, H., Itaya, T., Ogata, K., 1984. An age determination by K–Ar method. Bull. Hiruzen Res. Inst., Okayama Univ. of Sci. (9), 19–38 (in Japanese with English abst.).

Nishimura, Y., 1998. Geotectonic subdivision and areal extent of the Sangun belt, Inner Zone of southwest Japan. J. Metam. Geol. 16, 129–140.

Nishimura, Y., Itaya, T., Isozaki, Y., Kmeya, A., 1989. Deositional age and metamorphic history of 220 Ma high P/T type metamorphic rocks: an example of the Nishiki-cho area, Yamaguchi Prefecture, Southwest Japan. Mem. Geol. Soc. Japan (33), 143–166.

Oh, C.W., Choi, S.G., Song, S.H., Kim, S.W., 2004. Metamorphic evolution of the Baekdong metabasite in the Hongseong area, South Korea and its relationship with the Sulu Collision belt of China. Gondwana Res. 7, 809–816.

Okay, A.I., 1995. Paragonite eclogites from Dabie Shan, China: re-equilibration during exhumation? J. Metamorph. Geol. 13, 449–460.

Ota, K., Itaya, T., 1989. Radiometric ages of granitic and metamorphic rocks in the Hida metamorphic belt, central Japan. Bull. Hiruzen Res. Inst., Okayama Univ. of Sci. 15, 1–12 (in Japanese with English abst.).

Powell, R., Holland, T.J.B., Worley, B., 1998. Calculating phase diagram involving solid solutions via non-linear equations with examples using THERMOCALC. J. Metamorph. Geol. 16, 577–588.

Sano, Y., Hidaka, H., Terada, K., Shimizu, H., Suzuki, M., 2000. Ion microprobe U–Pb zircon geochronology of the Hida gneiss; finding of the oldest minerals in Japan. Geochem. J. 34, 35–153.

Schneider, J., Bosch, D., Monie, P., Guillot, S., Carcia-Casco, A., Lardeaux, J.M., Luis Torres-Roldan, R., Millan Trujillo, G., 2004. Origin and evolution of the Escambray Massif (central Cuba): an example of HP/LT rocks exhumed during intraoceanic subduction. J. Metamorph. Geol. 22, 227–247.

Shibata, K., Ito, M., 1978. Isotopic ages of schist from the Asahidake–Shiroumadake area, Hida Mountains. J. Japan. Ass. Mineral. Petrol. Econ. Geol. 73, 1–4.

Shibata, K., Nozawa, T., 1968. K–Ar age of Omi schist, Hida Mountains. Japan. Bull. Geol. Surv. Japan (19), 243–246.

Shibata, K., Nizawa, T., Uchiumi, S., 1980. K–Ar ages from Hida marginal belt. Report. Scientific Project 'Hida–Gaien Belt', Grant-in-aid for Scientific Res. (A), vol. 1, pp. 1–14 (in Japanese).

Sohma, T., Akiyama, S., 1984. Geological structure and lithofacies in the central part of the Hida metamorphic belt. J. Geol. Soc. Japan 90, 609–628.

Steigher, R., Jäger, E., 1977. Subcommission on geochronology: convention on the use of decay constants in geo- and cosmochronology. Earth Planet. Sci. Lett. 35, 359–362.

Suzuki, K., Adachi, M., 1994. Middle Precambrian detrital monazite and zircon from the Hida gneiss in the Oki-Dogo Island, Japan: their origin and implication for the correlation of the basement of Southwest Japan and Korea. Tectonophysics 235, 277–292.

Suzuki, M., Nakazawa, S., Osakabe, T., 1989. Tectonic development of the Hida belt—with special reference to its metamorphic history and Late Carboniferous to Triassic orogenies. Mem. Geol. Soc. Japan (33), 1–10 (in Japanese with English abst.).

Suzuki, H., Isozaki, Y., Itaya, T., 1990. Tectonic superposition of the Kurosegawa terrane upon the Sanbagawa metamorphic belt in the eastern Shikoku, Southwest Japan—K–Ar ages of weakly metamorphosed rocks ion the northeastern Kamikatsu Town , Tokushima Prefecture. J. Geol. Soc. Japan. 96, 145–153 (in Japanese with English abst.).

Tazawa, J., 2004. Palaeozoic and Mesozoic tectonics of the Hida Gaien Belt, central Japan: overview. J. Geol. Soc. Japan 110, 567–579 (in Japanese with English Abst.).

Tsujimori, T., 1995. Staurolite-bearing sillimanite schist cobble from the Upper Jurassic Tetori Group in the Kuzuryu area, Hida Mountains, central Japan. J. Geol. Soc. Japan 101, 971–977.

Tsujimori, T., 2002. Prograde and retrograde $P–T$ paths of the Late Paleozoic glaucophane eclogite from the Renge metamorphic belt, Hida Mountains, Southwestern Japan. Int. Geol. Rev. 44, 797–818.

Tsujimori, T., Itaya, T., 1999. Blueschist-facies metamorphism during Paleozoic orogeny in southwestern Japan: phengite K–Ar ages of blueschist-facies tectonic blocks in a serpentinite mélange beneath Early Paleozoic Oeyama ophiolite. Isl. Arc 8, 190–205.

Tsujimori, T., Ishiwatari, A., Banno, S., 2000a. Eclogitic glaucophane schist from the Yunotani valley in Omi Town, the Renge metamorphic belt, the Inner Zone of southwestern Japan. J. Geol. Soc. Japan 106, 353–362 (in Japanese with English abst.).

Tsujimori, T., Nishina, K., Ishiwatari, A., Itaya, T., 2000b. 443–403 Ma kyanite-bearing epidote amphibolite from the Fuko Pass metacumulate in the Oeyama area, the Inner Zone of southwestern Japan. J. Geol. So. Japan 106, 646–649 (in Japanese with English abst.).

Tsujimori, T., Liou, J.G., 2004a. Ecologite-facies mineral inclusions in clinozoisite from Palaezoic blueschist, central Chugoku Mountains, SW Japan: Evidence of regional eclogite-facies matamorphism. Int. Geol. Rev. 46, 215–232.

Tsujimori, T., Liou, J.G., 2004b. Metamorphic evolution of kyanite–staurolite-bearing epidote-amphibolitic rocks from the Early Paleozoic Oeyama belt, SW Japan. J. Metamorph. Geol. 22, 301–314.

Tomaschek, F., Kennedy, A.K., Villa, I.M., Lagos, M., Ballhaus, C., 2003. Zircons from Syros, Cyclades, Greece—recystallization and mobilization of zircon during high-pressure metamorphism. J. Petrol. 44, 1977–2002.

Webb, L.E., Hacker, B.R., Ratschbacher, L., Dong, S., 1999. Tectonics of high and ultrahigh-pressure rocks in the Qinling–Dabie orogen: $^{40}Ar/^{39}Ar$ thermochronologic constraints on deformation and cooling history. Tectonophysics 18, 621–638.

Yokoyama, K., 1985. Ultramafic rocks in the Hida Marginal Zone. Mem. Natn. Sci. Mus., Tokyo (18), 5–18.

Yamada, K., 1967. Stratigraphy and geologic structure of the Paleozoic formations in the Upper Kuzuryu River district, Fukui Prefecture, central Japan. Sci. Rep. Kanazawa Univ. (12), 185–207.